Journal of Sound and Vibration (2000) **232**(2), 331–354
doi:10.1006/jsvi.1999.2746, available online at http://www.idealibrary.com on IDEAL®

SIMPLIFICATION OF FINITE ELEMENT MODELS FOR STRUCTURES HAVING A BEAM-LIKE BEHAVIOUR

S. Corn, J. Piranda and N. Bouhaddi

Laboratoire de Mécanique Appliquée R. Chaléat, U.F.R. Sciences et Techniques, 24, *Chemin de I'Epitaphe*, 25030 *Besançon Cedex, France*

(*Received* 6 *April* 1998, *and in final form* 2 *September* 1999)

A method for simplifying finite element models of structures having a beam-like global dynamical behaviour is presented. This method is based on the use of a general uniform beam finite element formulation. It takes into account both transverse shear effects and dynamical coupling between bending and torsion due to the fact that mass centres and shear centres do not always coincide. For that purpose, we develop a condensation method for reducing any shell model into an equivalent beam, as well as a technique for automatically identifying the corresponding set of beam parameters. The method is applied to several illustrate examples that demonstrate its ability to simplify finite element models for many kinds of sophisticated structures having a beam-like predominant behaviour.

1. INTRODUCTION

The coupling between CAD and finite element software allows models of complex structures to be generated, and yield a nearly perfect representation of their topology. Applied to industrial cases, refined meshes can lead to accurate models that match the real dynamical characteristics of the structure. However, such precise discretizations of a whole structure results in very large finite element models which are not practically exploitable in an industrial context. To be usable, the model has to be simplified while preserving its dynamical behaviour in a given frequency band.

Several methods can be applied in order to get reduced models. The most popular are condensation and component mode synthesis methods [1–3]. They are based on the decomposition of the global complex structure into several substructures having a simpler geometry, which are individually condensed and then assembled. The approach proposed below is based on the observation that many industrial structure components have in fact a beam-like behaviour for the first modes. For example, models for car bodies contain many beam-like substructures which are usually finely meshed with shell elements (ribs, pillars, stiffeners, etc.). In this case, if appropriate "equivalent beam" properties for each subpart can be identified, it can naturally lead to a significant reduction of the degrees of freedom (dof). The resulting condensed models can then be assembled with the remaining global structure.

A simple and efficient condensation method is described in this paper. It allows all of the physical parameters of the equivalent beam model to be automatically obtained. This method is well adapted to the simplification of hollow straight structures for which shear centre and mass centre do not generally coincide.

We will first present the explicit formulation of the beam finite element that will be used. This is a straight beam element based on Timoshenko hypotheses [4] and which takes into

0022-460X/00/170331 + 24 $35.00/0

account the coupling between bending and torsion due to the fact that the shear and mass centres may not have the same location.

Secondly, a parameterization of the problem is defined. It allows one to express elementary matrices of the equivalent model for general configurations in which the locations of the mass and shear centres and the principal directions are unknown.

The last step explains how to identify automatically the characteristic parameters of the equivalent beam, whatever the shape of the cross-section. A significant reduction of the number of d.o.f.s is obtained for the reduced model while preserving the dynamical global behaviour with respect to the initial one in the low-frequency domain. The efficiency and the representability of the method are illustrated using several numerical tests.

2. DESCRIPTION OF THE GENERAL BEAM ELEMENT

2.1. CONTINUOUS MODEL

Let us consider a straight beam defined by the length L and the constant cross-section A. In each cross-section, two characteristic geometric points can be defined [5]: the mass centre G and the shear centre C (which is the invariant point of the cross-section displacement when the beam is submitted to an external torque). For uniform cross-section beams, the neutral axis (locus of points G) and the elastic axis (locus of points C) are parallel. Let us define a Cartesian reference frame (x_p, y_p, z_p) where x_p is parallel to the elastic axis and y_p and z_p are the principal bending directions (Figure 1). This reference frame is centred at C_1, whose location is supposed to be known. For a homogeneous structure, these directions are also the principal inertia directions of the solid.

Let $(\bar{y}_G, \bar{z}_G)$ be the coordinates of G with respect to C in each cross-section S. Let M be a point at the co-ordinates (x, y, z). The classical definitions for the inertia are

$$\int_S (y - \bar{y}_G)\,\mathrm{d}S = 0,$$

$$\int_S (z - \bar{z}_G)\,\mathrm{d}S = 0,$$

$$\int_S (y - \bar{y}_G)(z - \bar{z}_G)\,\mathrm{d}S = 0,$$

$$\int_S (y - \bar{y}_G)^2\,\mathrm{d}S = I_z,$$

$$\int_S (z - \bar{z}_G)^2\,\mathrm{d}S = I_y, \tag{1}$$

where I_z (respectively I_y) is the second moment of area with respect of z_p (respectively y_p).

According to classical kinematical hypotheses, if warping effects are neglected each cross-section has a rigid-body motion. The displacement field (u, v, w) at point M then depends on the displacement (u_C, v_C, w_C) at point C and on the rotation of the cross-section $(\theta_x, \theta_y, \theta_z)$. When the points C and G are not at the same location, a static coupling occurs between bending, torsion and extension effects if the kinematic variables are all expressed at

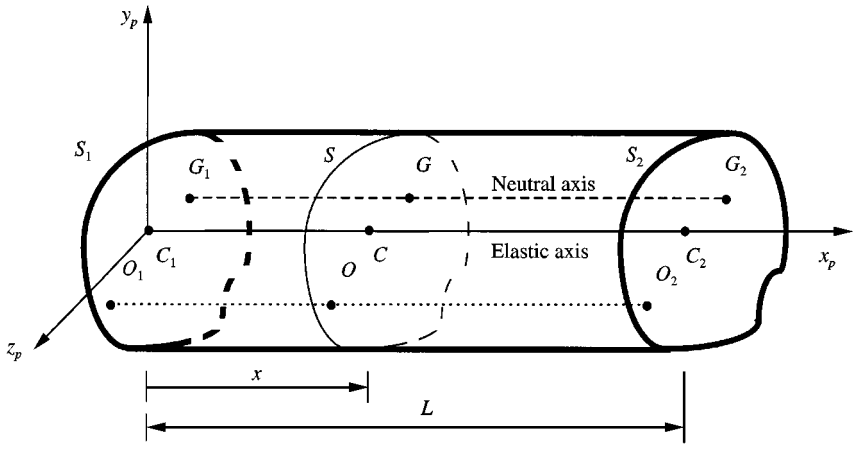

Figure 1. Straight beam with constant cross-section.

the same point (C or G). But, these effects can be separated under static conditions if the displacement u_G associated with the extension is expressed with respect to G and the others with respect to C. Then the set of displacements on each cross-section can be written as

$$u = u_G + (z - \bar{z}_G)\theta_y - (y - \bar{y}_G)\theta_z,$$

$$v = v_C - z\theta_x,$$

$$w = w_C + y\theta_x. \tag{2}$$

The stress field related to the displacements is defined by the normal stress σ_{xx} and the transverse stresses σ^s_{xy} and σ^s_{xz} (respectively σ^t_{xy} and σ^t_{xz}) due to shear (respectively to torsion). The forces acting on a cross section are:

normal force at G:

$$N = \int_S \sigma_{xx}\,\mathrm{d}S,$$

shear forces:

$$T_y = \int_S \sigma^s_{xy}\,\mathrm{d}S,$$

$$T_z = \int_S \sigma^s_{xz}\,\mathrm{d}S, \tag{3}$$

bending moments at G:

$$M_y = \int_S (z - \bar{z}_G)\sigma_{xx}\,\mathrm{d}S,$$

$$M_z = -\int_S (y - \bar{y}_G)\sigma_{xx}\,\mathrm{d}S,$$

torsion moment at C:

$$M_x = \int_S (y\sigma_{xz}^t - z\sigma_{xy}^t)\,\mathrm{d}S.$$

Taking into account equations (1) and (2), and according to Timoshenko theory [4], the following force–displacement relations can be obtained for an elastic isotropic material:

$$N = EA\frac{\partial u_G}{\partial x},$$

$$T_y = k_y \mu A\left(\frac{\partial v_C}{\partial x} - \theta_z\right),$$

$$T_z = k_z \mu A\left(\frac{\partial w_C}{\partial x} + \theta_y\right),$$

$$M_y = EI_y\frac{\partial \theta_y}{\partial x},$$

$$M_z = EI_z\frac{\partial \theta_z}{\partial x},$$

$$M_x = \mu J\frac{\partial \theta_x}{\partial x}, \tag{4}$$

where E is the elasticity modulus, μ the shear modulus, k_y and k_z are the shear factors [6] and J is the Saint-Venant torsion rigidity constant calculated in C.

The strain energy SE of the beam of volume V is expressed as

$$SE = \frac{1}{2}\int_V \sigma^{\mathrm{T}}\varepsilon\,\mathrm{d}V \tag{5}$$

or using the previous relationship (3):

$$SE = \frac{1}{2}\int_0^L \left(N\frac{\partial u_G}{\partial x} + T_y\left(\frac{\partial v_C}{\partial x} - \theta_z\right) + T_z\left(\frac{\partial w_C}{\partial x} + \theta_y\right)\right.$$

$$\left. + M_y\frac{\partial \theta_y}{\partial x} + M_z\frac{\partial \theta_z}{\partial x} + M_x\frac{\partial \theta_x}{\partial x}\right)\mathrm{d}x. \tag{6}$$

Using equations (4), the following expression of the energy versus the displacements can be given:

$$SE = \frac{1}{2}\int_0^L \left(EA\left(\frac{\partial u_G}{\partial x}\right)^2 + k_y\mu A\left(\frac{\partial v_C}{\partial x} - \theta_z\right)^2 + k_z\mu A\left(\frac{\partial w_C}{\partial x} + \theta_y\right)^2\right.$$

$$\left. + EI_y\left(\frac{\partial \theta_y}{\partial x}\right)^2 + EI_z\left(\frac{\partial \theta_z}{\partial x}\right)^2 + \mu J\left(\frac{\partial \theta_x}{\partial x}\right)^2\right)\mathrm{d}x. \tag{7}$$

It clearly shows that no static coupling occurs between the different deformation effects.

Moreover, the kinetic energy KE of the beam is given by

$$KE = \frac{1}{2}\int_V \rho(\dot{u}^2 + \dot{v}^2 + \dot{w}^2)\,\mathrm{d}V, \tag{8}$$

where ρ is the mass density of the material.

Using equations (1) and (2) leads to

$$KE = \frac{1}{2}\int_0^L \rho(A\dot{u}_G^2 + A\dot{v}_C^2 + A\dot{w}_C^2 + I_y\dot{\theta}_y^2 + I_z\dot{\theta}_z^2$$

$$+ I_C\dot{\theta}_x^2 - 2\bar{z}_G A\dot{v}_C\dot{\theta}_x + 2\bar{y}_G A\dot{w}_C\dot{\theta}_x)\,\mathrm{d}x \tag{9}$$

with $I_C = I_y + I_z + (\bar{y}_G^2 + \bar{z}_G^2)A$.

The cross-terms $\dot{v}_C\dot{\theta}_x$ and $\dot{w}_C\dot{\theta}_x$ in equation (9) shows that bending and torsion are dynamically coupled [7]. It can be noticed that the terms related to the rotational inertia are not neglected.

The equations governing the motion will not be presented here since the aim of the presentation concerns mainly the finite element formulation for the beam previously defined. These equations have been established in detail by Bishop and Price [8] in the case of the straight beam having a symmetric cross-section.

2.2. DISCRETE MODEL

Let us consider a beam finite element having two nodes and 6-d.o.f. per node. The nodal variables are defined by

$$\mathbf{q}_p = [u_{G_1}\, u_{G_2}\, v_{C_1}\, \theta_{z_1}\, v_{C_2}\, \theta_{z_2}\, w_{C_1}\, \theta_{y_1}\, w_{C_2}\, \theta_{y_2}\, \theta_{x_1}\, \theta_{x_2}]^{\mathrm{T}} \tag{10}$$

(the subscript $i = 1, 2$ are related to the end i of the element).

Classically, we use for each kind of deformation a polynomial interpolation corresponding to the static solution. This leads to a linear interpolation for both the tension evaluated in G and the torsion, and a cubic interpolation for the bending.

The elementary mass and stiffness matrices of the beam finite element are derived from the elementary energies. So, the stiffness matrix $\mathbf{K}^p$ is deduced from the strain energy, see equation (7). This matrix can be decomposed into several submatrices (whose expressions are given in Appendix A) in the following manner:

$$\mathbf{K}^p = \left[\begin{array}{c|c|c|c} \mathbf{K}^{u_G} & \mathbf{0} & \mathbf{0} & \mathbf{0} \\ \hline & \mathbf{K}^{v_C} & \mathbf{0} & \mathbf{0} \\ \hline & & \mathbf{K}^{w_C} & \mathbf{0} \\ \hline & sym & & \mathbf{K}^{\theta_x} \end{array}\right] \in \mathbf{R}^{12,12}. \tag{11}$$

Using the same interpolation functions [9, 10] as in statics, the elementary mass matrix $\mathbf{M}^p$ is obtained. The partition is similar to the one defined for the stiffness matrix (see

Appendix B):

$$\mathbf{M}^p = \begin{bmatrix} \mathbf{M}^{u_G} & \mathbf{0} & \mathbf{0} & \mathbf{0} \\ & \mathbf{M}^{v_C} & \mathbf{0} & \mathbf{M}^{v_C\theta_x} \\ & & \mathbf{M}^{w_C} & \mathbf{M}^{w_C\theta_x} \\ & sym & & \mathbf{M}^{\theta_x} \end{bmatrix} \in \mathbf{R}^{12,12}. \tag{12}$$

However, it is useful to express the elementary matrices with respect to the nodal unknown q_C corresponding to the nodes C and ordered in the following manner:

$$\mathbf{q}_C = [u_{C_1}\ v_{C_1}\ w_{C_1}\ \theta_{x_1}\ \theta_{y_1}\ \theta_{z_1}\ u_{C_2}\ v_{C_2}\ w_{C_2}\ \theta_{x_2}\ \theta_{y_2}\ \theta_{z_2}]^{\mathrm{T}}. \tag{13}$$

According to the hypothesis of non-deformation of the cross-sections, a matrix describing the geometric relationship between the longitudinal displacements expressed in G and the nodal unknowns q_C can be given using the following relation deduced from equation (2):

$$\begin{bmatrix} u_{G_1} \\ u_{G_2} \end{bmatrix} = \begin{bmatrix} 1 & 0 & 0 & 0 & \bar{z}_G - \bar{y}_G & 0 & 0 & 0 & 0 & 0 & 0 \\ 0 & 0 & 0 & 0 & 0 & 0 & 1 & 0 & 0 & 0 & \bar{z}_G & -\bar{y}_G \end{bmatrix} \mathbf{q}_C. \tag{14}$$

Applying this transformation to matrices $\mathbf{K}^p$ and $\mathbf{M}^p$, reordered with respect to the d.o.f.s defined in equation (13), one obtains finally the elementary matrices $\mathbf{K}^p_C$ and $\mathbf{M}^p_C$ for the general straight beam element expressed with respect to (C_1, C_2) in the principal inertia axes. This element takes into account both the shear effect and the eccentricity of the shear centre with respect to the mass centre. Similar results have been proposed by Dubigeon and Kim [11] in the case of a finite element taking into account the warping due to the torsion by using a 7-d.o.f. per node beam element.

3. IDENTIFICATION OF THE EQUIVALENT ELEMENT

3.1. PARAMETERIZATION

In practice, girders may have a closed cross-section of any shape. The principal bending directions (y_p, z_p) defining the local axes and the inside co-ordinates of C (y_C, z_C) and G (y_G, z_G) are *a priori* unknown. As such, the previous finite element formulation is not general enough to allow the parameterization of the equivalent beam model. It must be completed in such a way that it can be expressed with respect to two arbitrary points, and in any orientation of the global computational axes.

For this, we define two points O_1 and O_2 such that O_1 (respectively O_2) belongs to the end section S_1 (respectively S_2) plane, O_1O_2 being parallel to the direction x_p of the beam (see Figure 1). From now on, O_1 is defined as the origin of the global reference axes (see Figure 2). According to the theory of beams, each cross-section has a rigid-body motion, particularly the terminal sections S_1 and S_2. A rigid-body transformation $\mathbf{T}_{C_i\ (i=1,2)}$ can be defined, allowing the displacement of the point C_i of co-ordinates (y_C, z_C) to be expressed with respect to the displacements q_{O_i} of the

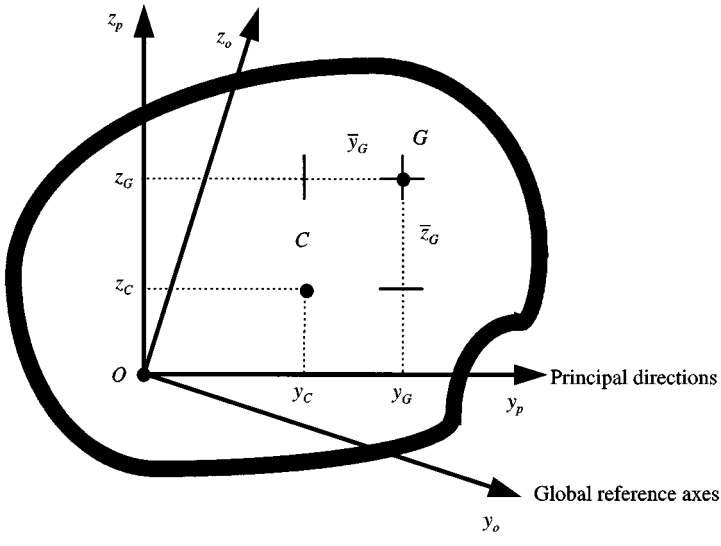

Figure 2. Location of parameters in a cross-section.

point O_i in the following manner:

$$\mathbf{T}_{C_1} = \mathbf{T}_{C_2} = \left[\begin{array}{c|ccc} & 0 & z_C & -y_C \\ \mathbf{I}_3 & -z_C & 0 & 0 \\ & y_C & 0 & 0 \\ \hline \mathbf{0} & & \mathbf{I}_3 & \end{array}\right] \in \mathbf{R}^{6,6}. \tag{15}$$

The transformation of the nodes (C_1, C_2) into (O_1, O_2) is then defined by

$$\begin{bmatrix} \mathbf{q}_{C_1} \\ \mathbf{q}_{C_2} \end{bmatrix} = \left[\begin{array}{c|c} \mathbf{T}_{C_1} & \mathbf{0} \\ \hline \mathbf{0} & \mathbf{T}_{C_2} \end{array}\right] \begin{bmatrix} \mathbf{q}_{O_1} \\ \mathbf{q}_{O_2} \end{bmatrix} \quad \text{also written: } \mathbf{q}_C \triangleq \mathbf{T}_C \mathbf{q}_O. \tag{16}$$

The stiffness and mass elementary matrices $\mathbf{K}_O^p$ and $\mathbf{M}_O^p$ expressed with respect to (O_1, O_2) in the principal axes are

$$\mathbf{K}_O^p = \mathbf{T}_C^{\mathrm{T}} \mathbf{K}_C^p \mathbf{T}_C, \qquad \mathbf{M}_O^p = \mathbf{T}_C^{\mathrm{T}} \mathbf{M}_C^p \mathbf{T}_C. \tag{17}$$

Moreover, it can be shown after a few manipulations that the 12-d.o.f.s stiffness matrix $\mathbf{K}_O^p$ can be partitioned into submatrices, each of them depending on four 3-d.o.f.s basic matrices $\mathbf{K}_1, \mathbf{K}_2, \mathbf{Q}_1$ and $\mathbf{Q}_2$.

So, $\mathbf{K}_O^p$ can be expressed as

$$\mathbf{K}_O^p = \left[\begin{array}{c|c|c|c} \mathbf{K}_1 & \mathbf{K}_1\mathbf{Q}_1 & -\mathbf{K}_1 & -\mathbf{K}_1\mathbf{Q}_2 \\ \hline & \mathbf{Q}_1^{\mathrm{T}}\mathbf{K}_1\mathbf{Q}_1 + \mathbf{K}_2 & -\mathbf{Q}_1^{\mathrm{T}}\mathbf{K}_1 & -\mathbf{Q}_1^{\mathrm{T}}\mathbf{K}_1\mathbf{Q}_2 - \mathbf{K}_2 \\ \hline & & \mathbf{K}_1 & \mathbf{K}_1\mathbf{Q}_2 \\ \hline & sym & & \mathbf{Q}_2^{\mathrm{T}}\mathbf{K}_1\mathbf{Q}_2 + \mathbf{K}_2 \end{array}\right]. \tag{18}$$

The basic matrices $\mathbf{K}_1$ and $\mathbf{K}_2$ are defined by

$$\mathbf{K}_1 = \begin{bmatrix} \dfrac{EA}{L} & 0 & 0 \\ 0 & \dfrac{12EI_z}{(1+\phi_y)L^3} & 0 \\ 0 & 0 & \dfrac{12EI_y}{(1+\phi_z)L^3} \end{bmatrix}, \qquad \mathbf{K}_2 = \begin{bmatrix} \dfrac{\mu J}{L} & 0 & 0 \\ 0 & \dfrac{EI_y}{L} & 0 \\ 0 & 0 & \dfrac{EI_z}{L} \end{bmatrix}. \tag{19}$$

It depends on all the parameters of the classical beam formulation. It can be noticed that $\phi_y = 12EI_z/k_yA\mu L^2$ and $\phi_z = 12EI_y/k_zA\mu L^2$ correspond to the shear effects correction. They vanish to zero for slender beams.

The matrices $\mathbf{Q}_1$ and $\mathbf{Q}_2$ depend only on the co-ordinates of C and G expressed with respect to the principal frame centred at O (Figure 2). It leads to

$$\mathbf{Q}_1 = \begin{bmatrix} 0 & z_G & -y_G \\ -z_C & 0 & L/2 \\ y_C & -L/2 & 0 \end{bmatrix}, \qquad \mathbf{Q}_2 = \begin{bmatrix} 0 & z_G & -y_G \\ -z_C & 0 & -L/2 \\ y_C & L/2 & 0 \end{bmatrix} \tag{20}$$

with

$$\begin{Bmatrix} y_G = y_C + \bar{y}_G \\ z_G = z_C + \bar{z}_G \end{Bmatrix}.$$

In order to obtain the most general formulation of the equivalent beam, the previous elementary matrices have to be expressed in an abritrary direction (y_0, z_0) of the global computational reference frame. Let $\mathbf{\Theta}$ be the rotation matrix defining the principal axes (y_p, z_p) with respect to the global reference frame. The orthogonal transformation matrix $\mathbf{R}$ is classically defined by

$$\mathbf{R} = \begin{bmatrix} \mathbf{\Theta} & \vdots & \vdots & \vdots \\ \cdots & \cdots & \cdots & \cdots \\ \vdots & \mathbf{\Theta} & \vdots & \vdots \\ \cdots & \cdots & \cdots & \cdots \\ \vdots & \vdots & \mathbf{\Theta} & \vdots \\ \cdots & \cdots & \cdots & \cdots \\ \vdots & \vdots & \vdots & \mathbf{\Theta} \end{bmatrix}, \quad \mathbf{\Theta}^{\mathrm{T}}\mathbf{\Theta} = \mathbf{I}_3. \tag{21}$$

The stiffness and mass matrices $\mathbf{K}_O$ and $\mathbf{M}_O$ of the equivalent element expressed with respect to (O_1, O_2) can be defined as

$$\mathbf{K}_O = \mathbf{R}^{\mathrm{T}}\mathbf{K}_O^p\mathbf{R}, \qquad \mathbf{M}_O = \mathbf{R}^{\mathrm{T}}\mathbf{M}_O^p\mathbf{R}. \tag{22}$$

Partitioning the matrix $\mathbf{K}_O$ according to equation (18), leads to the top left 3-d.o.f.s submatrix $\mathbf{\Theta}^{\mathrm{T}}\mathbf{K}_1\mathbf{\Theta}$.

Since $\mathbf{K}_1$ defined by equation (19) is a diagonal matrix, it can be easily deduced that the principal axes (y_p, z_p) are the eigenvectors of this submatrix.

All the parameters of the analytical equivalent beam model being thus defined, we present now a procedure for their identification.

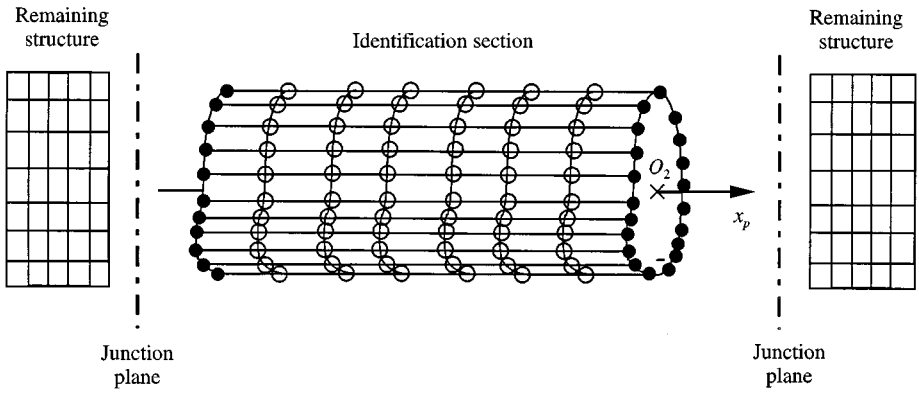

Figure 3. Guyan condensation of the shell model; ●, master nodes; ○, slave nodes.

3.2. CONDENSATION AND PARAMETRIC IDENTIFICATION

The proposed method is applied to a straight girder part finely meshed using shell elements. The basic hypothesis consists in assuming that this substructure has a beam-like behaviour inside the whole structure for its first eigenmodes.

Let $\tilde{\mathbf{K}}$ and $\tilde{\mathbf{M}}$ be the assembled numerical stiffness and mass matrices of the refined model for this substructure.

In a first step, Guyan condensation [1] is applied to this model (Figure 3). Therefore, the d.o.f.s are divided in two subsets: the master d.o.f.s (to be preserved) related to the junctions nodes (suffix j) and the slave nodes (to be removed) related to the internal nodes (suffix i).

The vector of the nodal unknowns $\mathbf{y}$ and the matrices $\tilde{\mathbf{K}}$ and $\tilde{\mathbf{M}}$ are then distributed in the following manner:

$$\mathbf{y} = \begin{bmatrix} \mathbf{y}_j \\ \mathbf{y}_i \end{bmatrix}, \quad \tilde{\mathbf{K}} = \begin{bmatrix} \tilde{\mathbf{K}}_{jj} & \tilde{\mathbf{K}}_{ji} \\ \tilde{\mathbf{K}}_{ji}^{\mathrm{T}} & \tilde{\mathbf{K}}_{ii} \end{bmatrix}, \quad \tilde{\mathbf{M}} = \begin{bmatrix} \tilde{\mathbf{M}}_{jj} & \tilde{\mathbf{M}}_{ji} \\ \tilde{\mathbf{M}}_{ji}^{\mathrm{T}} & \tilde{\mathbf{M}}_{ii} \end{bmatrix}. \tag{23}$$

The dynamic equilibrium of the substructure submitted to junctions forces is written as

$$(\tilde{\mathbf{K}} - \omega^2 \tilde{\mathbf{M}})\mathbf{y} = \mathbf{F}, \tag{24}$$

where $\mathbf{F} = \begin{bmatrix} \mathbf{F}_j \\ 0 \end{bmatrix}$ denotes the junctions forces.

The transformation $\mathbf{T}_g$ is deduced from the static Guyan condensation as

$$\mathbf{y} = \begin{bmatrix} \mathbf{I}_j \\ -\tilde{\mathbf{K}}_{ii}^{-1}\tilde{\mathbf{K}}_{ji}^{\mathrm{T}} \end{bmatrix} \mathbf{y}_j \triangleq \mathbf{T}_g \mathbf{y}_j. \tag{25}$$

Equation (24) can then be expressed in the condensed form as

$$(\mathbf{T}_g^{\mathrm{T}} \tilde{\mathbf{K}} \mathbf{T}_g - \omega^2 \mathbf{T}_g^{\mathrm{T}} \tilde{\mathbf{M}} \mathbf{T}_g)\mathbf{y}_j = \mathbf{F}_j. \tag{26}$$

Equation (26) describes the condensed Guyan model expressed on the junctions d.o.f.s.

Then, according to the hypothesis of non-deformability of cross-sections, a rigid-body relation can be established between O_1 (respectively O_2) and each node N_1^j of S_1 (respectively N_2^j of S_2):

$$\underset{(6,1)}{\mathbf{y}_{N_1^j}} = \underset{(6,6)}{\mathbf{T}_{N_1^j}} \underset{(6,1)}{\mathbf{q}_{O_1}}, \qquad \mathbf{y}_{N_2^j} = \mathbf{T}_{N_2^j}\mathbf{q}_{O_2}. \tag{27}$$

So, the following transformations can be obtained for each set of nodes in the end sections:

$$\mathbf{T}_{S_1} = \begin{bmatrix} \mathbf{T}_{N_1^1} \\ \vdots \\ \mathbf{T}_{N_1^j} \\ \mathbf{T}_{N_1^{j+1}} \\ \vdots \\ \mathbf{T}_{N_1^{n_1}} \end{bmatrix} \quad \text{and} \quad \mathbf{T}_{S_2} = \begin{bmatrix} \mathbf{T}_{N_2^1} \\ \vdots \\ \mathbf{T}_{N_2^j} \\ \mathbf{T}_{N_2^{j+1}} \\ \vdots \\ \mathbf{T}_{N_2^{n_2}} \end{bmatrix}. \tag{28}$$

The complete transformation matrix $\mathbf{T}_S$ between the N junctions d.o.f.s $\mathbf{y}_j$ of the terminal sections and $\mathbf{q}_O$ is defined by

$$\mathbf{y}_j = \begin{bmatrix} \mathbf{T}_{S_1} & \vdots & \mathbf{0} \\ \cdots & \cdots & \cdots \\ \mathbf{0} & \vdots & \mathbf{T}_{S_2} \end{bmatrix} \mathbf{q}_O \triangleq \mathbf{T}_S \mathbf{q}_O. \tag{29}$$

$$(N,1) \quad (N,12) \quad (12,1)$$

It can be noticed that the computation cost is significantly reduced by applying simultaneously the double transformation $\mathbf{T}_g\mathbf{T}_S$.

Finally, the numerical matrices $\tilde{\mathbf{K}}_O$ and $\tilde{\mathbf{M}}_O$ corresponding to the 12-d.o.f.s condensed model, expressed in (O_1, O_2) for any orientation with respect to the reference axes are given as.

$$\tilde{\mathbf{K}}_O = \mathbf{T}_S^{\mathrm{T}}\mathbf{T}_g^{\mathrm{T}}\tilde{\mathbf{K}}\mathbf{T}_g\mathbf{T}_S, \qquad \tilde{\mathbf{M}}_O = \mathbf{T}_S^{\mathrm{T}}\mathbf{T}_g^{\mathrm{T}}\tilde{\mathbf{M}}\mathbf{T}_g\mathbf{T}_S. \tag{30}$$

The identification procedure consists in computing the terms of the analytical matrix $\mathbf{K}_O$ previously defined (22) using the numerical values of those of the condensed matrix $\tilde{\mathbf{K}}_O$.

Hence, the principal axes of the beam (y_p, z_p) are identified using the previously defined submatrix $\mathbf{\Theta}^{\mathrm{T}}\mathbf{K}_1\mathbf{\Theta}$ of the numerical matrix $\tilde{\mathbf{K}}_O$, by solving a simple (3×3) eigenproblem. Then, the matrix $\mathbf{R}$ defined by equation (21) is evaluated. $\tilde{\mathbf{K}}_O^p$ is obtained using the inverse relation

$$\tilde{\mathbf{K}}_O^p = \mathbf{R}\tilde{\mathbf{K}}_O\mathbf{R}^{\mathrm{T}}. \tag{31}$$

The numerical values corresponding to the submatrices $\mathbf{K}_1, \mathbf{K}_1\mathbf{Q}_1$ and $\mathbf{Q}_1^{\mathrm{T}}\mathbf{K}_1\mathbf{Q}_1 + \mathbf{K}_2$ defined by equation (18) are then determined, and also the numerical computation of the basic matrices $\mathbf{K}_1$, $\mathbf{Q}_1$ and $\mathbf{K}_2$ defined by equations (19, 20). The positions of the shear centre $C(y_C, z_C)$ and of the mass centre $G(y_G, z_G)$ are obtained using $\mathbf{Q}_1$, and the six generic parameters A, J, I_y, I_z, k_y, k_z of the equivalent beam model are identified using $\mathbf{K}_1$ and $\mathbf{K}_2$.

The equivalent mass density ρ is separately determined using the 6-d.o.f. matrix obtained by condensing statistically the mass matrix $\tilde{\mathbf{M}}_O$ on only one of the two nodes of the beam. Indeed, the double transformation $\mathbf{T}_g\mathbf{T}_S$ defined by relations (25) and (29) preserves the total

mass of the model. So, the thus obtained rigid-body inertia matrix gives the total mass $\tilde{m}_T$ of the initial model. The mass density ρ is deduced from the equation

$$\tilde{m}_T = \rho AL. \tag{32}$$

Practically, the simplified equivalent beam model is obtained by meshing the whole structure length using an adequate number of beam finite elements of characteristics identified with this method.

4. NUMERICAL RESULTS

The proposed method for the reduction of finite element models has been tested on several straight structures having a beam-like behaviour. Numerical results are obtained for structures having different cross-section shapes and finely meshed using 6-d.o.f. per node shell elements. The material is assumed to be homogeneous and isotropic and to have the following properties:

Elasticity modulus: $E = 2{\cdot}1 \times 10^{11}$ N/m^2.
Shear modulus: $\mu = 8{\cdot}077 \times 10^{10}$ N/m^2.
Mass density: $\rho = 7800$ kg/m^3.

4.1. STRUCTURE WITH A RECTANGULAR CROSS-SECTION

The tested structure is a straight tube, 1 m long, having a rectangular cross-section (Figure 4). According to the symmetry of the cross section, the principal bending axes (y_p, z_p) are known and the characteristic points C and G are collocated with the point O. The initial shell meshing is based on four divisions along each side and 20 divisions along the length. It leads to a 2016 d.o.f. finite element model.

Table 1 gives the characteristic parameters of the equivalent beam. For such a simple cross-section geometry, the theoretical values are known [12, 6]. A very good agreement between the theoretical values and those identified by using the proposed method can be seen.

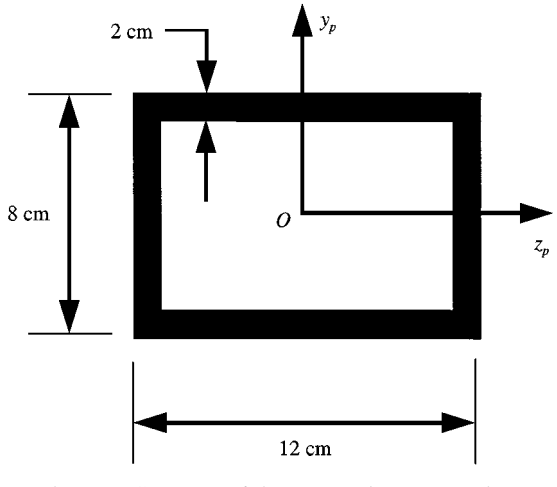

Figure 4. Geometry of the rectangular cross-section.

TABLE 1

Equivalent beam characteristics

Parameters	Theoretical value	Identified value
A (m^2)	$8{\cdot}000 \times 10^{-3}$	$8{\cdot}036 \times 10^{-3}$
J (m^4)	$1{\cdot}843 \times 10^{-5}$	$1{\cdot}964 \times 10^{-5}$
I_y (m^4)	$1{\cdot}786 \times 10^{-5}$	$1{\cdot}745 \times 10^{-5}$
I_z (m^4)	$9{\cdot}866 \times 10^{-6}$	$9{\cdot}592 \times 10^{-6}$
k_y	0·32	0·36
k_z	0·55	0·60
ρ (kg/m^3)	7800	7765
E (N/m^2)	$2{\cdot}1 \times 10^{11}$	—
μ (N/m^2)	$8{\cdot}077 \times 10^{10}$	—

TABLE 2

Eigenfrequencies—accuracy of the equivalent model: $e\ (\%) = 100\ (f - f_R)/f_R$

	Shell model 2016-d.o.f.s	Equivalent beam model 126-d.o.f.s				
		Theoretical parameters		Identified parameters		
Mode no.	Reference f_R (Hz)	f (Hz)	e (%)	f (Hz)	e (%)	Mode nature
1	593·11	598·00	0·82	594·88	0·29	Bending 1 (xy)
2	782·94	787·77	0·62	784·25	0·16	Bending 1 (xz)
3	1366·0	1313·1	− 3·87	1375·9	0·72	Torsion 1
4	1432·0	1431·1	− 0·06	1445·8	0·96	Bending 2 (xy)
5	1866·7	1859·9	− 0·36	1872·5	0·31	Bending 2 (xz)
6	2401·8	2411·5	0·40	2468·9	2·79	Bending 3 (xy)

TABLE 3

CPU times comparison for the "rectangular cross-section" structure

	CPU time (s)	
	Initial model	Equivalent model
Parameters identification	—	8·8
Six eigenmodes computation	19·1	0·6

In order to validate the equivalent model, we give in Table 2 the frequencies of the first eigenmodes of the free–free beam model built using the parameters given in Table 1 compared to the one of the refined model. The simplified model is meshed using 20 equivalent beams which gives 126-d.o.f.s compared to the 2016-d.o.f.s of the initial model. The model used for the beam is the previously defined Timoshenko formulation.

It can be seen that even though the equivalent beam model has a very small size compared to that of the refined model (reduction of up to 90%), the first eigenmodes of the

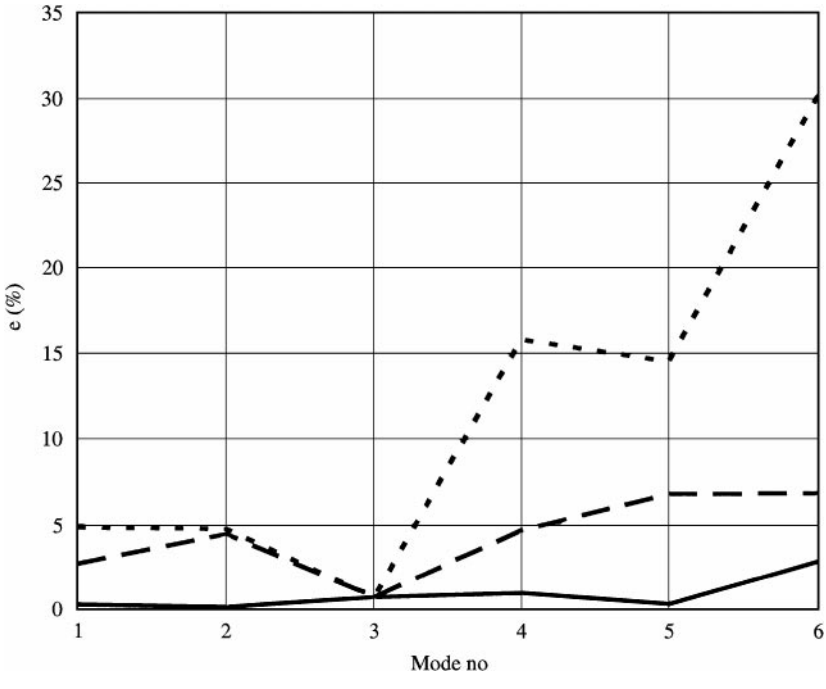

Figure 5. Comparison of the accuracy for different beam formulations: —— Timoshenko, - - - - Bernoulli, – – – mixed.

structure are well represented. A significant reduction of the CPU time can be noticed for the eigenvalues computation, which is divided by 30 (see Table 3). Moreover, using the identified values of the parameters instead of the theoretical ones leads to an accuracy of the same order.

Figure 5 compares the eigenfrequencies of the initial model to those obtained with a 126-d.o.f.s simplified model using the following different formulations for beam bending:

— Timoshenko model (stiffness $\mathbf{K}_C^p$ and $\mathbf{M}_C^p$ previously defined).
— Bernoulli model (shear and rotation inertia removed from the matrices $\mathbf{M}_C^p$ and $\mathbf{K}_C^p$).
— Mixed model (shear and rotation inertia removed only from the matrix $\mathbf{M}_C^p$).

The identified parameters given in Table 1 are used.

On the one hand, Figure 5 shows clearly that the Timoshenko formulation is the one that gives the best results for all the beam-like eigenmodes. On the other hand, the Bernoulli formulation overestimates the frequencies and leads to significant errors that increase with the mode number (except for the third one, which is a torsion mode). This phenomena is drastically amplified for short beams [13, 14]. The mixed formulation gives intermediate accuracy results. It can be noticed that this mixed formulation is the one used by the software NASTRAN (CBAR and CBEAM elements).

4.2. STRUCTURE WITH A "DELTA" CROSS-SECTION

The structure is a straight 3 m long beam having a "delta" cross-section (Figure 6). The shell finite element mesh has eight divisions along each side and 30 divisions along the length.

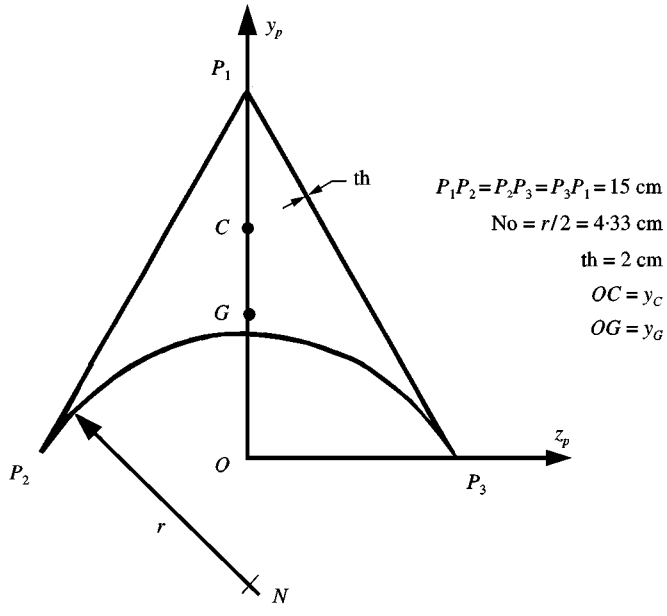

Figure 6. Geometry of the "delta" cross-section.

TABLE 4

Equivalent beam properties

Parameters	Identified value
y_C (cm)	8·21
y_G (cm)	5·10
A (m^2)	$9{\cdot}638 \times 10^{-3}$
J (m^4)	$5{\cdot}921 \times 10^{-6}$
I_y (m^4)	$1{\cdot}934 \times 10^{-5}$
I_z (m^4)	$1{\cdot}231 \times 10^{-5}$
k_y	0·49
k_z	0·51
ρ (kg/m^3)	7783
E (N/m^2)	$2{\cdot}1 \times 10^{11}$
μ (N/m^2)	$8{\cdot}077 \times 10^{10}$

For such a shape of the cross-section, some of the beam parameters (for example the shear factors) cannot be easily worked out. The whole set given in Table 4 has been identified using the proposed method.

The accuracy of the equivalent model is tested under clamped–free boundary conditions (cantilever beam). The initial model has 4464-d.o.f.s, which represents 24 times the number of d.o.f.s of the simplified model (186-d.o.f.s). Since the points C and G are not coincident, there exists a dynamic coupling between the bending in the plane $x_p z_p$ and the torsion about x.

Table 5 reports the results obtained from the proposed model, with the dynamic coupling between bending and torsion taken into account or not. It is evident that accounting for the coupling gives very good results in a large frequency band while neglecting this coupling

TABLE 5

Eigenfrequencies—accuracy of the equivalent model: $e\ (\%) = 100\ (f - f_R)/f_R$

Mode no.	Shell model 4464-d.o.f.s	Equivalent beam model 186-d.o.f.s			
		With coupling		Without coupling	
	Reference f_R (Hz)	f (Hz)	e (%)	f (Hz)	e (%)
1	11·519	11·517	− 0·02	11·517	− 0·02
2	14·394	14·391	− 0·02	14·422	0·19
3	71·082	71·299	0·30	71·299	0·30
4	86·499	86·771	0·31	88·720	2·56
5	118·33	117·81	− 0·44	102·03	− 13·7
6	194·55	195·91	0·69	195·91	0·69
7	230·23	232·26	0·88	241·53	4·91
8	357·40	356·05	− 0·37	306·38	− 14·2
9	369·88	374·05	1·12	374·05	1·12
10	418·16	424·94	1·62	455·76	8·99
11	432·90	432·91	0·00	432·91	0·00
12	590·26	599·38	1·54	599·38	1·54
13	606·65	606·01	− 0·10	511·57	− 15·7
14	630·08	645·51	2·45	718·16	14·0
15	848·17	864·64	1·94	864·64	1·94

leads to unacceptable errors. The model without coupling is thus unable to represent correctly the dynamic behaviour of the structure.

Furthermore, Figure 7 represents the "projection matrix" **P**, which is defined as follows. Let $\mathbf{Y}_1$ be the modal basis of the eigenvectors obtained with the model which accounts for the coupling, and $\mathbf{Y}_0$ be the basis of those obtained with the "no coupling" model. Each column of **P** consists of the factors of the linear combination between the corresponding vector of $\mathbf{Y}_1$ and those of $\mathbf{Y}_0$, which can be written as

$$\mathbf{Y}_1 = \mathbf{Y}_0 \mathbf{P}. \tag{33}$$

Since $\mathbf{Y}_0$ is a truncated basis, relation (33) has to be considered in a least-squares sense. Then, the projection matrix **P** can be defined by

$$\mathbf{P} = \mathbf{Y}_0^+ \mathbf{Y}_1, \tag{34}$$

where $\mathbf{Y}_0^+$ is the well-known Moore–Penrose pseudo-inverse matrix, defined from $\mathbf{Y}_0$ by

$$\mathbf{Y}_0^+ = (\mathbf{Y}_0^{\mathrm{T}} \mathbf{Y}_0)^{-1} \mathbf{Y}_0^{\mathrm{T}}. \tag{35}$$

A graphic representation of matrix **P**, as shown Figure 7, is used to highlight the modes for which the coupling between bending and torsion is particularly prominent (in this case, modes number 4, 5, 7,8, …).

However, in order to specify the nature of these modes, the displacement w for the bending along (z) and the displacement $\bar{y}_G \theta_x$ due to the torsion can be plotted on the same graph. We report in Figure 8 some typical results obtained for some of the first eigenmodes having a strong coupling (see Table 5). It can be noticed that, in this particular case, the number of nodes of any mode is not directly related to the mode number [15].

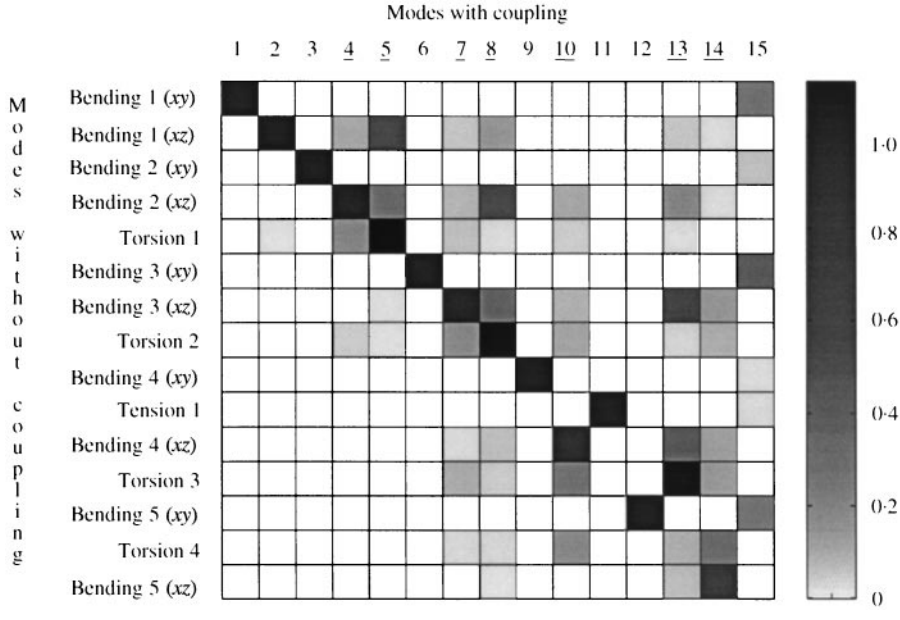

Figure 7. Projection matrix relating with and without coupling eigenmodes.

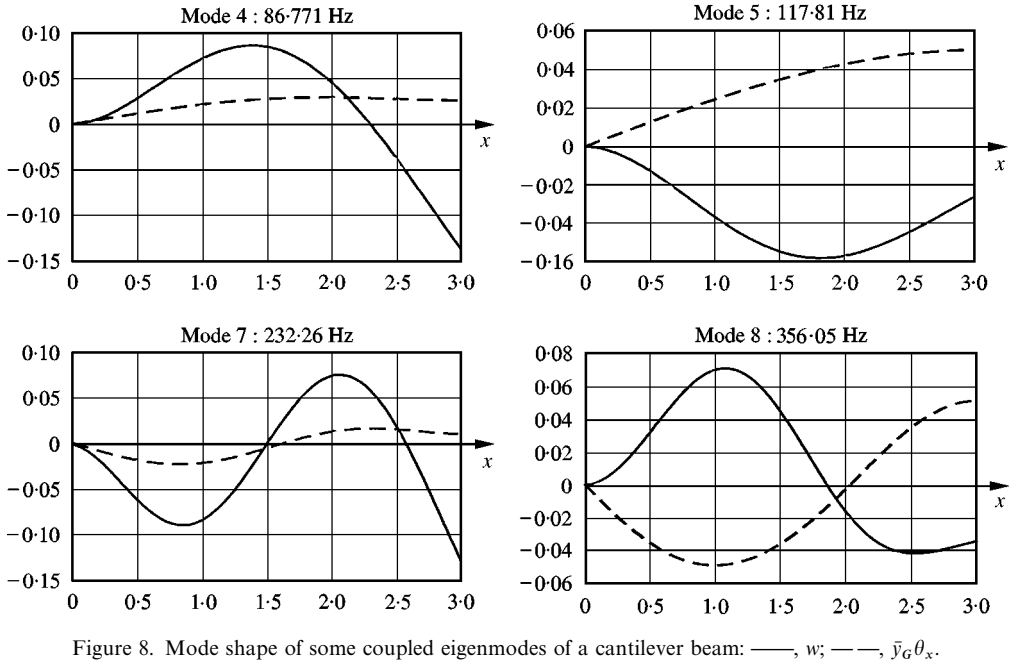

Figure 8. Mode shape of some coupled eigenmodes of a cantilever beam: ——, w; — —, $\bar{y}_G\theta_x$.

All these results demonstrate that the dynamic coupling between bending and torsion, which is taken into account in the proposed formulation, has a predominant effect on the dynamic behaviour of the structure and should not be neglected.

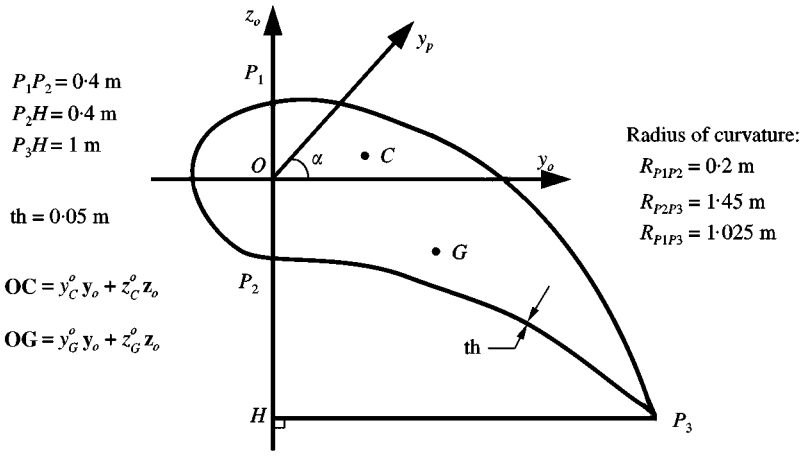

Figure 9. Geometry of the "aerofoil" cross-section.

TABLE 6

Equivalent beam properties

Parameters	Identified value
y_C^0 (m)	0·241
z_C^0 (m)	0·031
y_G^0 (m)	0·424
z_G^0 (m)	− 0·157
α (deg)	63·7
A (m^2)	$1{\cdot}561 \times 10^{-1}$
J (m^4)	$9{\cdot}619 \times 10^{-3}$
I_y (m^4)	$2{\cdot}771 \times 10^{-2}$
I_z (m^4)	$3{\cdot}791 \times 10^{-3}$
k_y	0·14
k_z	0·78
ρ (kg/m^3)	7765
E (N/m^2)	$2{\cdot}1 \times 10^{11}$
μ (N/m^2)	$8{\cdot}077 \times 10^{10}$

4.3. STRUCTURE WITH AN "AEROFOIL" CROSS-SECTION

The considered structure is a 6 m long straight tube having an aerofoil cross-section (Figure 9). The initial meshing has eight divisions on each of the three semi-circles and 20 divisions along the length. The positions of the characteristic points C and G as well as the principal bending axes (y_p, z_p) are *a priori* unknown.

The proposed method allows the set of parameters of the equivalent beam to be identified. These parameters are given Table 6. The reduced model has 126-d.o.f.s compared to the 3024 d.o.f.s of the initial model (reduction ratio of up 95%).

Table 7 shows the frequencies obtained for these two models for the first eigenmodes of the cantilevered structure. The clamped–free structure has local deformations from the first eigenmodes onwards. In order to test its beam-like behaviour, the free end must be loaded. The structure is loaded on the shear center of the free end with a mass of 5×10^3 kg and an inertia of 5×10^4 kg m^2 in the three directions.

TABLE 7

Eigenfrequencies—accuracy of the equivalent model: $e\ (\%) = 100\ (f - f_R)/f_R$

Mode no.	Shell model 3024-d.o.f.s	Equivalent beam model 126-d.o.f.s		Mode nature
	f_R (Hz)	f (Hz)	e (%)	
1	5·211	5·212	0·02	Bending 1 (xy)
2	8·047	8·049	0·02	Bending-torsion
3	14·02	14·02	0·00	Bending 1 (xz)
4	17·26	17·27	0·05	Bending 2 (xy)
5	45·76	45·79	0·07	Bending 2 (xz)
6	64·69	67·87	4·92	Local deformations
7	102·2	135·3	32·4	Local deformations

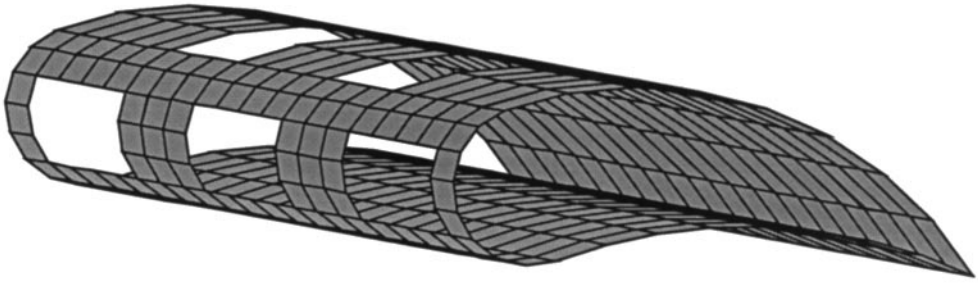

Figure 10. "Aerofoil" structure with holes.

The results obtained for the five first modes confirm the good accuracy of the proposed equivalent model despite of the substantial reduction of the size of the model. From the sixth eigenmode onwards the errors are quite large due to local deformations that obviously cannot be represented by the equivalent beam model for which each cross-section is supposed to have a rigid-body motion.

The numerical simulations which are presented until now concern straight homogeneous structures with a constant cross-section. Some existing software allow the determination of the beam parameters using a specific finite element discretization of the cross-section or integral equation techniques [16]. These methods are usable only if the cross-section has a constant shape along the axis of the beam.

The proposed method is more general since the identification of the parameters is based on the elastic beam behaviour of the structure and not on a computation on the cross-section shape. So, it can be applied to structures having local perturbations but yet a global beam behaviour. This advantage is demonstrated in the following numerical case where the structure is the previous aerofoil profile tube, with holes as shown in Figure 10. Despite of the discontinuity of the centreline, the proposed method gives a good prediction of the global behaviour of the structure.

Table 8 gives the parameters identified using the proposed method. In the case where the section is not constant, these parameters can be considered as "average" parameters. The beam model thus obtained is an equivalent model in the sense of a homogenization of the geometrical characteristics. It can be noticed that the positions of C and G, as well as the

TABLE 8

Equivalent beam properties

Parameters	Identified value
y_C^0 (m)	0·848
z_C^0 (m)	− 0·318
y_G^0 (m)	0·495
z_G^0 (m)	− 0·216
α (deg)	64·5
A (m^2)	$1{\cdot}285 \times 10^{-1}$
J (m^4)	$2{\cdot}651 \times 10^{-3}$
I_y (m^4)	$2{\cdot}095 \times 10^{-2}$
I_z (m^4)	$2{\cdot}852 \times 10^{-3}$
k_y	0·09
k_z	0·56
ρ (kg/m^3)	8539
E (N/m^2)	$2{\cdot}1 \times 10^{11}$
μ (N/m^2)	$8{\cdot}077 \times 10^{10}$

TABLE 9

Eigenfrequencies—accuracy of the equivalent model: $e\ (\%) = 100\ (f - f_R)/f_R$

Mode no.	Shell model 2868 d.o.f.s	Equivalent beam model 126-d.o.f.s		Mode nature
	f_R (Hz)	f (Hz)	e (%)	
1	4·203	4·211	0·20	Bending-torsion
2	4·555	4·558	0·05	Bending 1 (xy)
3	12·22	12·24	0·20	Bending 1 (xz)
4	14·78	14·86	0·51	Bending 2 (xy)
5	39·14	39·45	0·78	Bending 2 (xz)
6	47·08	50·43	7·10	Local deformations
7	78·54	98·89	25·9	Local deformations

bending and torsional moments of inertia, have been significantly modified compared to the values of the unperforated model given in Table 6.

In order to validate the homogenization, the eigenmodes have been computed with the same loads as the one used for the uniform structure. The results obtained for the first eigenfrequencies, by using the equivalent beam model and the fine mesh, are listed in Table 9. The equivalent model gives in this case as accurate results as the ones before, even if this structure has local discontinuities. It must be noticed that a classical method based only on a computation from the cross-section shape would be utterly inadequate, as it can be seen by comparing the eigenfrequencies given in Tables 7 and 9.

5. CONCLUDING REMARKS

The simplification of finite element models for structures having a beam-like behaviour leads to a drastic reduction in size (currently 90%) while preserving the global dynamic

properties (eigenfrequencies, mode shapes) at frequencies where the cross-sections remain undeformed. The proposed method takes advantage of a formal calculation which provides an analytical expression for the stiffness and mass matrices of a general Timoshenko beam that takes into account the dynamic coupling between bending and torsion as a result of the possible offset between the shear centre and the mass centre. The procedure is based on a double condensation of the stiffness matrix leading to a 12-d.o.f.s numerical matrix expressed in the same reference axes as that of the analytical matrix. The following equivalent beam parameters are then identified: principal directions, location of the mass and shear centres, second moments of area and torsional rigidity constant, shear factors, and equivalent mass density.

A wide variety of test results were presented and serve to illustrate the efficiency of the method. An important characteristic of this approach is that it preserves the physical meaning of the parameters to be identified. They can thus be used unambiguously in either optimization or updating procedures.

The proposed methodology is the result of a preliminary study concerning the simplification of complex sub-components of car bodies, that are generally assembled from stamped and spot-welded sheets reinforced with ribs which are modelled by combining CAD and finite element calculations. This generally provides an accurate representation of the dynamic behaviour but a very high cost (a few thousand d.o.f.s for the finite element model of such sub-component). This model must be simplified if calculations on the entire car are to be performed at a reasonable cost. A generalization of this method is currently under study for structures having variable cross-sections and curvatures.

REFERENCES

1. R. J. GUYAN 1965 *American Institute of Aeronautics and Astronautics Journal* **3**, 380. Reduction of stiffness and mass matrices.
2. R. R. CRAIG, J. and M. C. C. BAMPTON 1968 *American Institute of Aeronautics and Astronautics Journal* **6**, 1313–1319. Coupling of substructure for dynamic analysis.
3. R. H. MACNEAL 1971 *Computers and Structures* **1**, 581–601. A hybrid method of component mode synthesis.
4. S. P. TIMOSHENKO 1922 *Philosophical Magazine* **43**, 125–131. On the transverse vibrations of bars of uniform cross sections.
5. J. L. BATOZ and G. DHATT 1990 *Modélisation des Structures par Éléments Finis*, *Vol.* 2, *Poutres et Plaques.* Paris: Hermes.
6. G. R. COWPER 1966 *Journal of Applied Mechanics*, *ASME* **33**, 335–340. The shear coefficient in Timoshenko's beam theory.
7. W. L. HALLAUER and R. Y. L. LIU 1982 *Journal of Sound and Vibration* **85**, 105–113. Beam bending-torsion dynamic stiffness method for calculation of exact vibration modes.
8. R. E. D. BISHOP and W. G. PRICE 1977 *Journal of Sound and Vibration* **50**, 469–477. Coupled bending and twisting of a Timoshenko beam.
9. J. S. PRZEMIENIECKI 1968 *Theory of Matrix Structural Analysis.* New York: McGraw-Hill.
10. R. DAVIS, R. D. HENSHELL and G. B. WARBURTON 1972 *Journal of Sound and Vibration* **22**, 475–487. A Timoshenko beam element.
11. S. DUBIGEON and C. B. KIM 1982 *Journal of Sound and Vibration* **81**, 255–270. A finite element for the study of coupled bending-prevented torsion of a straight beam.
12. R. D. BLEVINS 1979 *Formulas for Natural Frequency and Mode Shape.* New York: Van Nostrand Reinhold.
13. D. GAY 1979 *Ph.D. Thesis*, *Toulouse*, *France*. Influence des effets secondaires sur les vibrations de flexion et de torsion des poutres.
14. S. CORN, N. BOUHADDI and J. PIRANDA 1997 *Journal of Sound and Vibration* **201**, 353–363. Transverse vibrations of short beams: finite element models obtained by a condensation method.
15. J. R. BANERJEE 1989 *International Journal for Numerical Methods in Engineering* **28**, 1283–1298. Coupled bending-torsional dynamic stiffness matrix for beam elements.

16. C. CZEKAJSKI, D. GAY and A. POTIRON 1984 *Proceedings of the 2nd International Conference on Recent Advances in Structural Dynamics Vol.* 1, 119–125. A boundary element program for the calculation of coupled flexure-torsion constants for beams of any cross section shape.

APPENDIX A: STIFFNESS MATRIX OF THE BEAM ELEMENT

Matrix associated to tension in G:

$$\mathbf{K}^{u_G} = \frac{EA}{L}\begin{matrix} \\ u_{G_1} \\ u_{G_2} \end{matrix}\begin{matrix} \begin{matrix} u_{G_1} & u_{G_2} \end{matrix} \\ \begin{bmatrix} 1 & -1 \\ -1 & 1 \end{bmatrix} \end{matrix}.$$

Matrix associated to torsion in C:

$$\mathbf{K}^{\theta_x} = \frac{\mu J}{L}\begin{matrix} \\ \theta_{x_1} \\ \theta_{x_2} \end{matrix}\begin{matrix} \begin{matrix} \theta_{x_1} & \theta_{x_2} \end{matrix} \\ \begin{bmatrix} 1 & -1 \\ -1 & 1 \end{bmatrix} \end{matrix}.$$

Matrix associated to bending in C:

$$\mathbf{K}^{v_C} = \frac{EI_z}{(1+\phi_y)L^3}\begin{matrix} \\ v_{C_1} \\ \theta_{z_1} \\ v_{C_2} \\ \theta_{z_2} \end{matrix}\begin{matrix} \begin{matrix} v_{C_1} & \theta_{z_1} & v_{C_2} & \theta_{z_2} \end{matrix} \\ \begin{bmatrix} 12 & 6L & -12 & 6L \\ & (4+\phi_y)L^2 & -6L & (2-\phi_y)L^2 \\ & & 12 & -6L \\ & sym & & (4+\phi_y)L^2 \end{bmatrix} \end{matrix}$$

with $\phi_y = 12EI_z/k_y A\mu L^2$,

$$\mathbf{K}^{w_C} = \frac{EI_y}{(1+\phi_z)L^3}\begin{matrix} \\ w_{C_1} \\ \theta_{y_1} \\ w_{C_2} \\ \theta_{y_2} \end{matrix}\begin{matrix} \begin{matrix} w_{C_1} & \theta_{y_1} & w_{C_2} & \theta_{y_2} \end{matrix} \\ \begin{bmatrix} 12 & 6L & -12 & -6L \\ & (4+\phi_z)L^2 & 6L & (2-\phi_z)L^2 \\ & & 12 & 6L \\ & sym & & (4+\phi_z)L^2 \end{bmatrix} \end{matrix}$$

with $\phi_z = 12EI_y/k_z A\mu L^2$.

APPENDIX B: MASS MATRIX OF THE BEAM ELEMENT

Matrix associated to tension in G:

$$\mathbf{M}^{u_G} = \frac{\rho AL}{6}\begin{matrix} \\ u_{G_1} \\ u_{G_2} \end{matrix}\begin{matrix} \begin{matrix} u_{G_1} & u_{G_2} \end{matrix} \\ \begin{bmatrix} 2 & 1 \\ 1 & 2 \end{bmatrix} \end{matrix}.$$

Matrix associated to torsion in C:

$$\mathbf{M}^{\theta_x} = \frac{\rho I_C L}{6}\begin{matrix} \\ \theta_{x_1} \\ \theta_{x_2} \end{matrix}\begin{matrix} \begin{matrix} \theta_{x_1} & \theta_{x_2} \end{matrix} \\ \begin{bmatrix} 2 & 1 \\ 1 & 2 \end{bmatrix} \end{matrix}$$

with $I_C = I_y + I_z + (\bar{y}_G^2 + \bar{z}_G^2)A$.

Matrices of coupling between bending and torsion in C:

$$\mathbf{M}^{v_C\theta_x} = \frac{\bar{z}_G \rho AL}{(1+\phi_y)} \begin{bmatrix} \theta_{x_1} & \theta_{x_2} & \\ -\left(\frac{7}{20}+\frac{1}{3}\phi_y\right) & -\left(\frac{3}{20}+\frac{1}{6}\phi_y\right) & v_{C_1} \\ -\left(\frac{1}{20}+\frac{1}{24}\phi_y\right) & -\left(\frac{1}{30}+\frac{1}{24}\phi_y\right) & \theta_{z_1}, \\ -\left(\frac{3}{20}+\frac{1}{6}\phi_y\right) & -\left(\frac{7}{20}+\frac{1}{3}\phi_y\right) & v_{C_2} \\ \left(\frac{1}{30}+\frac{1}{24}\phi_y\right) & \left(\frac{1}{20}+\frac{1}{24}\phi_y\right) & \theta_{z_2} \end{bmatrix}$$

with $\phi_y = 12EI_z/k_y A\mu L^2$,

$$\mathbf{M}^{w_C\theta_x} = \frac{\bar{y}_G \rho AL}{(1+\phi_z)} \begin{bmatrix} \theta_{x_1} & \theta_{x_2} & \\ \left(\frac{7}{20}+\frac{1}{3}\phi_z\right) & \left(\frac{3}{20}+\frac{1}{6}\phi_z\right) & w_{C_1} \\ -\left(\frac{1}{20}+\frac{1}{24}\phi_z\right) & -\left(\frac{1}{30}+\frac{1}{24}\phi_z\right) & \theta_{y_1}, \\ \left(\frac{3}{20}+\frac{1}{6}\phi_z\right) & \left(\frac{7}{20}+\frac{1}{3}\phi_z\right) & w_{C_2} \\ \left(\frac{1}{30}+\frac{1}{24}\phi_z\right) & \left(\frac{1}{20}+\frac{1}{24}\phi_z\right) & \theta_{y_2} \end{bmatrix}$$

with $\phi_z = 12EI_y/k_z A\mu L^2$.

Matrices associated to bending in C:

$$\mathbf{M}^{v_C} = \frac{\rho AL}{(1+\phi_y)^2}$$

$$\begin{bmatrix} v_{C_1} & \theta_{z_1} & v_{C_2} & \theta_{z_2} & \\ \left(\frac{13}{35}+\frac{7}{10}\phi_y+\frac{1}{3}\phi_y^2 + \frac{6}{5}r_z^2\right) & \left(\frac{11}{210}+\frac{11}{120}\phi_y+\frac{1}{24}\phi_y^2 + \left(\frac{1}{10}-\frac{1}{2}\phi_y\right)r_z^2\right)L & \left(\frac{9}{70}+\frac{3}{10}\phi_y+\frac{1}{6}\phi_y^2 - \frac{6}{5}r_z^2\right) & -\left(\frac{13}{420}+\frac{3}{40}\phi_y+\frac{1}{24}\phi_y^2 - \left(\frac{1}{10}-\frac{1}{2}\phi_y\right)r_z^2\right)L & v_{C_1} \\ & \left(\frac{1}{105}+\frac{1}{60}\phi_y+\frac{1}{120}\phi_y^2 + \left(\frac{2}{15}+\frac{1}{6}\phi_y+\frac{1}{3}\phi_y^2\right)r_z^2\right)L^2 & \left(\frac{13}{420}+\frac{3}{40}\phi_y+\frac{1}{24}\phi_y^2 - \left(\frac{1}{10}-\frac{1}{2}\phi_y\right)r_z^2\right)L & -\left(\frac{1}{140}+\frac{1}{60}\phi_y+\frac{1}{120}\phi_y^2 + \left(\frac{1}{30}+\frac{1}{6}\phi_y-\frac{1}{6}\phi_y^2\right)r_z^2\right)L^2 & \theta_{z_1} \\ & & \left(\frac{13}{35}+\frac{7}{10}\phi_y+\frac{1}{3}\phi_y^2 + \frac{6}{5}r_z^2\right) & -\left(\frac{11}{210}+\frac{11}{120}\phi_y+\frac{1}{24}\phi_y^2 + \left(\frac{1}{10}-\frac{1}{2}\phi_y\right)r_z^2\right)L & v_{C_2} \\ & sym & & \left(\frac{1}{105}+\frac{1}{60}\phi_y+\frac{1}{120}\phi_y^2 + \left(\frac{2}{15}+\frac{1}{6}\phi_y+\frac{1}{3}\phi_y^2\right)r_z^2\right)L^2 & \theta_{z_2} \end{bmatrix}$$

with $\phi_y = 12EI_z/k_yA\mu L^2$ and $r_z^2 = I_z/AL^2$,

$$\mathbf{M}^{w_C} = \frac{\rho AL}{(1+\phi_z)^2}$$

$$\begin{array}{cccc} w_{C_1} & \theta_{y_1} & w_{C_2} & \theta_{y_2} \end{array}$$

$$\begin{bmatrix}
\left(\frac{13}{35}+\frac{7}{10}\phi_z+\frac{1}{3}\phi_z^2\right) & -\left(\frac{11}{210}+\frac{11}{120}\phi_z+\frac{1}{24}\phi_z^2\right)L & \left(\frac{9}{70}+\frac{3}{10}\phi_z+\frac{1}{6}\phi_z^2\right) & \left(\frac{13}{420}+\frac{3}{40}\phi_z+\frac{1}{24}\phi_z^2\right)L \\
+\frac{6}{5}r_y^2 & +\left(\frac{1}{10}-\frac{1}{2}\phi_z\right)r_y^2 & -\frac{6}{5}r_y^2 & -\left(\frac{1}{10}-\frac{1}{2}\phi_z\right)r_y^2 \\
 & \left(\frac{1}{105}+\frac{1}{60}\phi_z+\frac{1}{120}\phi_z^2\right)L^2 & -\left(\frac{13}{420}+\frac{3}{40}\phi_z+\frac{1}{24}\phi_z^2\right)L & -\left(\frac{1}{140}+\frac{1}{60}\phi_z+\frac{1}{120}\phi_z^2\right)L^2 \\
 & +\left(\frac{2}{15}+\frac{1}{6}\phi_z+\frac{1}{3}\phi_z^2\right)r_y^2 & -\left(\frac{1}{10}-\frac{1}{2}\phi_z\right)r_y^2 & +\left(\frac{1}{30}+\frac{1}{6}\phi_z-\frac{1}{6}\phi_z^2\right)r_y^2 \\
 & & \left(\frac{13}{35}+\frac{7}{10}\phi_z+\frac{1}{3}\phi_z^2\right) & \left(\frac{11}{210}+\frac{11}{120}\phi_z+\frac{1}{24}\phi_z^2\right)L \\
 & & +\frac{6}{5}r_y^2 & +\left(\frac{1}{10}-\frac{1}{2}\phi_z\right)r_y^2 \\
 & sym & & \left(\frac{1}{105}+\frac{1}{60}\phi_z+\frac{1}{120}\phi_z^2\right)L^2 \\
 & & & +\left(\frac{2}{15}+\frac{1}{6}\phi_z+\frac{1}{3}\phi_z^2\right)r_y^2
\end{bmatrix}
\begin{array}{c} w_{C_1} \\ \theta_{y_1} \\ w_{C_2} \\ \theta_{y_2} \end{array}$$

with $\phi_z = 12EI_y/k_zA\mu L^2$ and $r_y^2 = I_y/AL^2$.

APPENDIX C: NOMENCLATURE

$\partial/\partial x$	derivative with respect to the variable x
$\dot{u} = \partial u/\partial t$	time derivative of function u
A	cross-sectional area of the beam
L	length of the beam element
(x_p, y_p, z_p)	principal bending directions
x	longitudinal axial co-ordinate
I_y	second moment of area with respect to the y_p-axis
I_z	second moment of area with respect to the z_p-axis
J	torsion rigidity constant
k_y	shear factor along y_p
k_z	shear factor along z_p
E	elasticity modulus
μ	shear modulus
ρ	mass density
ε	strain tensor
σ	stress tensor
SE	strain energy
KE	kinetic energy
$(\bar{y}_G, \bar{z}_G)$	location of mass centre G with respect to shear centre C in principal axes
d.o.f.s	degrees of freedom
$\mathbf{H}^{\mathrm{T}}$	transpose of matrix $\mathbf{H}$
$\mathbf{H}^+ = (\mathbf{H}^{\mathrm{T}}\mathbf{H})^{-1}\mathbf{H}^{\mathrm{T}}$	Moore–Penrose pseudo-inverse of matrix $\mathbf{H}$
$\mathbf{I}_3$	(3×3) identity matrix
$\mathbf{K}$	stiffness matrix of the beam finite element
$\mathbf{M}$	mass matrix of the beam finite element
$\mathbf{K}^p$	stiffness matrix of the beam finite element in the principal axes

$\mathbf{M}^p$	mass matrix of the beam finite element in the principal axes
$\mathbf{K}_C$	stiffness matrix of the beam finite element expressed at point C
$\mathbf{M}_C$	mass matrix of the beam finite element expressed at point C
ω	circular frequency of vibration (rad/s)
f	frequency of vibration (Hz)